Microcomb Source Based on InP DFB / Si3N4 Microring Butt-Coupling

Sylvain Boust, Houssein El Dirani, Laurène Youssef, Yannick Robert, Alexandre Larrue, Camille Petit-Etienne, Eric Vinet, Sebastien Kerdiles, Erwine Pargon, Mickael Faugeron, et al.

Microcomb source based on InP DFB / Si_3N_4 microring butt-coupling

Sylvain Boust, Houssein El Dirani, Laurène Youssef, Yannick Robert, Alexandre Larrue, Camille Petit-Etienne, Eric Vinet, Sébastien Kerdiles, Erwine Pargon, Mickaël Faugeron, Marc Vallet, François Duport, Corrado Sciancalepore, and Frédéric van Dijk

Abstract—**In this paper, we demonstrate an integrated Kerr frequency comb source based on the butt-coupling between a III-V (InGaAsP/InP) DFB laser and a silicon nitride (Si_3N_4) microresonator. The maturity of our silicon platforms permits the fabrication of high-quality factor microresonators with parametric oscillation threshold as low as 300 µW. Combined with a high optical power semiconductor chip, it enables to build an integrated comb source that consumes less than 3 W of electrical power, in less than one cm^3. Our source emits an optical comb centered at 1576 nm with a 30 dB bandwidth measured to be 13.6 THz, and a repetition rate of 113.5 GHz. The radio frequency (RF) spectrum associated to the global 10 mW output optical power is characterized both at low frequency and at the beat note frequency, in order to distinguish unstable comb generation from stable comb generation. Finally, we reveal how our hybrid compact source can be used to generate 17-soliton crystal state that is a comb with a 2.04 THz line spacing.**

Index Terms—**Optical frequency comb, photonic integrated circuits, semiconductor lasers, silicon nitride.**

I. INTRODUCTION

OPTICAL frequency comb sources are key elements in a growing number of applications, such as optical metrology, optical clocks [1], ultra-fast ranging distance [2] or multiplexing in photonic communications [3]. Broad frequency combs can be generated by Kerr nonlinearity in microresonator [4], [5], but it requires a voluminous, expensive and power-hungry setup which limits the number of applications. However, the rapid progress in integrated photonic platforms has significantly boosted the interest and the research about compact comb sources. Since 2018 [6], [7], a few teams of scientists has succeeded to replace the cumbersome pump laser needed to generate a Kerr comb by a III-V chip. It solved the problems previously mentioned, but brought some inconveniences, namely a fairly weak input power and a low bandwidth of the comb.

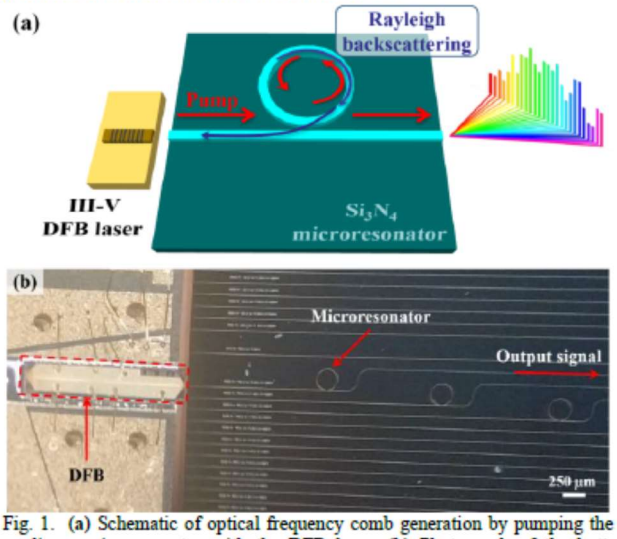

Fig. 1. **(a)** Schematic of optical frequency comb generation by pumping the nonlinear microresonator with the DFB laser. **(b)** Photograph of the butt-coupling. The output signal is extracted with a lens at the right of the passive waveguide (not visible on the picture). The two components are independent, and by the translation of the passive chip, different configurations of ring microresonators can be easily tested.

Our work is a continuation of these previous studies, as we present in this paper a compact comb source composed of a InGaAsP/InP distributed feedback DFB laser and a Si_3N_4 ring microresonator. Our passive microresonator is pumped with a continuous single mode DFB laser in a ring resonance which generates a Kerr frequency comb through parametric four-wave mixing [8]. Nonlinear effects occur at a low optical power in Si_3N_4 thanks to its significant nonlinear refractive index (compared to silica) and its ultra-low loss allowing microring resonators with very high-quality factor [9]. Many setups take benefit from non-linear effects in Si_3N_4 for comb generation [10], [11] or supercontinuum generation [12], [13]. Here, we propose a compact source that can emit a comb with a 13.6 THz 30 dB bandwidth and with a 10-mW global optical output power. Moreover, we observe a perfect soliton crystal, which presents 17 solitons evenly distributed in the microresonator. Such comb formations were realized without bulky stabilization methods such as Pound-Drever-Hall [14] or 'power kicking' setups [15]. Indeed, without an optical isolator between the pump and resonator, the Rayleigh backscattering generated in the microresonator is re-injected into the laser, leading to self-injection locking. Consequently,

Manuscript received Month Day, Year; (*Corresponding author: Sylvain Boust.*)

S. Boust, F. Duport, Y. Robert, A. Larrue, E. Vinet and F. van Dijk are with the III-V Lab, a joint laboratory between Nokia Bell Labs France, Thales Research and Technology France, and CEA-LETI, 91767 Palaiseau, France (e-mail: sylvain.boust@3-5lab.fr). S. Boust is also with Université Rennes, CNRS, Institut FOTON - UMR 6082, 35000 Rennes, France.

H. El Dirani, S. Kerdiles and C. Sciancalepore are with the CEA-LETI, 38000 Grenoble, France.

L. Youssef, C. Petit-Etienne, E. Pargon are with Université Grenoble Alpes, CNRS, LTM, 38000 Grenoble, France.

M. Vallet is with Université Rennes, CNRS, Institut FOTON - UMR 6082, 35000 Rennes, France.

M. Faugeron was with III-V Lab, 91767 Palaiseau, France. He is now with Thales Alenia Space, 31100 Toulouse, France.

frequency drifts due to thermal instabilities are self-compensated, which greatly eases the comb formation.

This paper is organized as follows. Section II presents the characteristics of the DFB laser. Section III first describes the fabrication process of the passive chip containing the microring resonator, and then presents the characterization results of the passive chip. The comb source is detailed in Section IV: we measure one optical comb at a fixed DFB laser bias current, and then we study the evolution of the system during a wavelength sweep. In Section V, we conclude and discuss the main challenges to overcome for potential applications.

II. HIGH POWER DFB LASER

The InGaAsP/InP DFB laser is designed to guarantee a single-mode operation while providing a sufficient power in order to reach the Kerr nonlinearity threshold in the ring resonator. The DFB laser is fabricated using a dual channel shallow ridge structure, as described in [16]. The laser cavity length is 1.75 mm. To ensure maximum output power and an optimal coupling with the passive chip, the back facet and the output facet of the laser are coated to be highly reflective and anti-reflective respectively. The lasing threshold is measured to be 81 mA and the output power ups to more than 200 mW, as shown in Fig. 2(a).

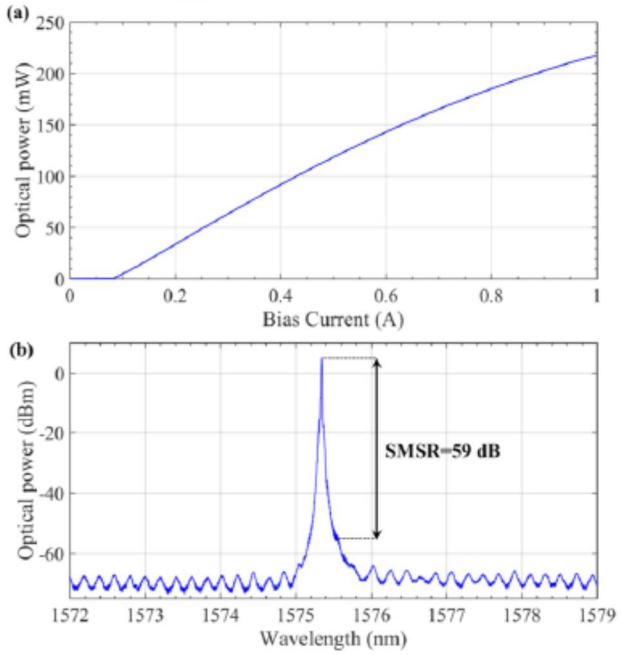

Fig. 2. (a) Optical power measurement at 25°C from the DFB laser. The output power was acquired with an integrating sphere. (b) Laser optical spectrum from the DFB laser chip acquired for a DFB bias current set at 647 mA, and a 23.7°C operating temperature. The 203 pm (24.6 GHz) local oscillation corresponds to the free spectral range of the DFB laser.

The laser output mode has an asymmetric shape: we measured a total divergence angle at $1/e^2$ of 20° × 60° (horizontal × vertical). This non-circular form is due to the specific design of the laser [16]. So as to minimize the coupling losses between the laser and the passive chip, we point out that the mode mismatch between the laser and the passive chip input should be as small as possible.

The lasing wavelength can be precisely tuned by changing the bias current (5 pm/mA for a temperature set around 25°C and a working bias current around 700 mA), which allows an easy scan of the microring's resonance. In Fig. 2(b), the measured spectrum of the laser exhibits a good side mode suppression ratio (SMSR) of 59 dB, which should circumvent possible perturbations of the frequency comb generation, such as, e.g., injection of the microring with a spurious side mode or mode hopping of the DFB. Moreover, the use of a single mode laser permits to easily control the experimental setup by enabling a continuous scan of the pump wavelength.

III. HIGH CONFINEMENT, LOW LOSS SILICON NITRIDE RING RESONATORS

A. Low-loss Si_3N_4 tightly confining waveguide

We start the fabrication process with a 3 µm-thick thermal oxidation of the 200 mm diameter silicon substrate to isolate the optical mode and avoid the leakage to the substrate. Then, following a tailored twist-and-grow deposition method [5], [17], 800 nm-thick silicon nitride film (Si_3N_4) is deposited by low pressure chemical vapor deposition (LPCVD). A 248 nm lithography on an ASML-300 stepper is performed using 820 nm-thick resist mask with a bottom anti-reflection coating (BARC). An inductively coupled plasma (ICP) reactor is used to etch the silicon nitride film. In order to increase the photoresist selectivity, the resist is cured by applying an HBr plasma [18]. We used an $Ar/Cl_2/O_2$ plasma process to open the BARC and the Si_3N_4 is then etched with a $CF_4/CHF_3/Ar$ plasma. The photoresist/BARC layers are removed using an O_2 plasma, and 1% HF dip. With the Si_3N_4 core waveguides exposed, we then apply a chemical-physical multistep annealing under successively H_2, O_2, and N_2 atmospheres [19]. In this way, the population of residual N-H bonds contained in the film drops drastically, avoiding detrimental absorption losses in the C-band. The silicon nitride circuits are then encapsulated using a two-step low-temperature oxide deposition including a 2 µm-thick silica cladding layer deposited at 400°C using high-density plasma-enhanced chemical vapor deposition (HDP-PECVD) technique to avoid voids formation, which is one of the main causes known for devices failure.

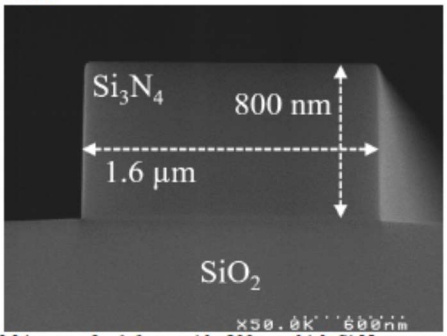

Fig. 3. SEM image of a 1.6 µm-wide 800 nm-thick Si_3N_4 waveguide profile after subtractive patterning exhibiting vertical sidewalls.

The Fig. 3 shows a SEM image of the Si_3N_4 waveguide before encapsulation in SiO_2. The propagation losses of

1.6 µm-wide × 800 nm-thick waveguides are then reduced from 80 dB/m [5] to just 10 dB/m thanks to the aforementioned process described in more detail in [19]. At the end of the process, a deep etch step has been used to form the chip facets, thus no additional facet polishing steps are required.

B. Si_3N_4/SiO_2 chip characteristics

The chip dimension is 20.0 × 21.3 mm. The microresonator used (see Fig. 1(a)) is a Si_3N_4 ring with a 200 µm radius. We design a 550 nm gap between the ring and the bus waveguide, which should result in a coupling close to critical. We simulate the dispersion of different waveguide widths (Fig. 4(a)) in order to design an anomalous dispersion across the C-band, which greatly eases frequency comb generation [6]. Thus, for our first configuration, we designed a 1.70 µm-wide and 800 nm-thick cross section for the resonator waveguide for the bus waveguide. Its lower dispersion will enable a larger comb generation, as it is predicted in [20]. However, this large cross section supports many transverse modes (4 TE and 4 TM modes). To address this issue, we designed an adiabatic taper at the beginning of the passive chip. It eases the coupling with the DFB laser and only the fundamental mode of the bus waveguide should be excited. Moreover, we placed a single mode S-bend (visible on the Fig. 1(a)) after the microresonator to suppress high order modes that may have been excited. The bus waveguide is 20 mm long. We measured the reflectivity and the transmission spectrum of the ring by using a high-resolution optical spectrum analyzer (OSA) from APEX Technologies (AP2043B model) with an integrated tunable laser source. We have looked only for transverse electric (TE) resonance since the DFB laser described in Section II is TE polarized.

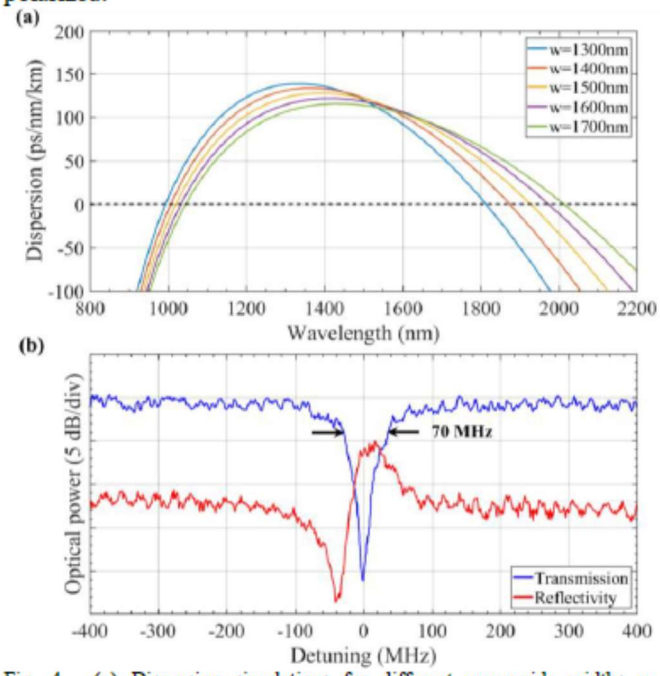

Fig. 4. **(a)** Dispersion simulations for different waveguide widths *w*. Increasing *w* enables low anomalous dispersion over a wider wavelength range. **(b)** Spectral response of the 200 µm radius microring, measured by a 0.04 pm (5 MHz) resolution OSA. The resonance was measured to be centered at 1575.31 nm.

The normalized transmission spectrum shows a 70 MHz resonance bandwidth (full width at half-maximum), meaning a loaded quality factor $Q_l = 2.8 \times 10^6$ (thus representing an intrinsic quality factor $Q_i = 5.6 \times 10^6$). Any small fabrication imperfections can easily induce a Rayleigh retrodiffusion in the microresonator which can be observed with the reflectivity curve in Fig. 5. Such a high-quality factor allows a very low parametric oscillation threshold for the comb generation. By using a classical formula (Eq. (5) of Ref. [21]), we estimate a theoretical 300 µW threshold.

By scanning the wavelength over 10 nm, we measured a 113.5 GHz (0.94 nm) free spectral range (FSR) of the microresonator, in agreement with a 200 µm radius. This FSR determines the line spacing associated to the generated frequency comb.

By injecting a test signal at the end of the passive waveguide, we measure the far-field of the passive waveguide before the microresonator. The full angle at $1/e^2$ is 22° × 34° (horizontal × vertical).

IV. HYBRID INTEGRATED OPTICAL COMB SOURCE

A. Hybrid InP-Si_3N_4/SiO_2 setup

To perform the butt-coupling between the DFB laser and the passive chip (Fig. 1), we use a dynamical alignment system with micrometric translation stages. Consequently, mechanical vibrations slightly affect the performances of our device. Conversely, the advantage is the possibility to easily test different ring configurations. The output signal is then collected with a lens, directly followed by a free-space optical isolator and coupled to a fiber by means of a collimator.

By computing the overlap of the measured far-field from the DFB laser and the microresonator, the minimum coupling intensity loss achievable on our setup is estimated around 0.6 dB to which 0.5 dB should be added due to the reflection at the Si_3N_4 chip input. We point out that the quality and the stability is strongly linked to the good alignment of the two components. Moreover the response of the pumped resonance is very dependent on the pump optical phase [22]. In our setup, we control this phase by carefully adjusting the air gap between the two components. Therefore, we take care to remove any spurious mechanical fluctuations in order to ensure pump phase stability during butt-coupling.

Since the microresonator is a passive component, the global electrical consumption is determined by that of the DFB laser and its cooling stage. In our case, it requires less than 3 W of electrical power.

In the two next parts, we will report studies performed on two similar microresonators whose widths and gaps with the bus waveguide are slightly different. This variation greatly affects their quality factor and slightly modifies their dispersion. As a consequence, the generated combs will be shown to be very different when these two microresonators are pumped.

B. Kerr frequency comb generation

With the microresonator presented in Fig. 4, we first study the generation of the most expected comb, which is a comb with a line spacing equal to the ring FSR (113.5 GHz).

When pumping the microresonator near a cavity mode, we generated a Kerr comb through cascaded parametric Four Wave Mixing (FWM) [8], as shown in Fig. 5(a). The Rayleigh backscattering in the microring observed in Fig. 4 induces an optical feedback in the DFB. It can enable a self-locking phenomenon for the DFB laser, which enhances the coupling stability of the pump wavelength with the microring resonance and a reduction of the pump linewidth [22].

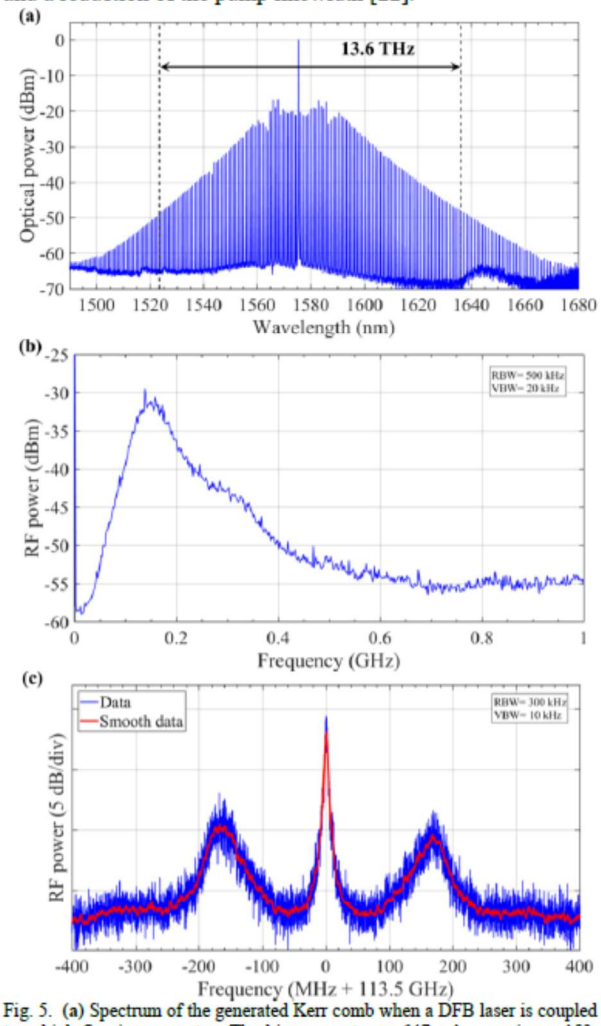

Fig. 5. **(a)** Spectrum of the generated Kerr comb when a DFB laser is coupled to a high-Q microresonator. The bias current was 647 mA, meaning a 153-mW output power. Nevertheless, due to the mode mismatch of the two components and the propagation losses in the Si_3N_4 bus waveguide, we estimate a maximum injection power of 110 mW. The actual injection power is lower due to alignment imperfection. During this measurement, our powermeter measured a corresponding optical power of 11 mW in the fiber. **(b)** RF spectrum measured of the Kerr comb detected by a 20 GHz photodiode. **(c)** Broad RF beatnotes measured at 113.5 GHz with a 70 GHz −3 dB bandwidth photodiode.

To match a resonance of the microresonator, we manually increased the pump wavelength. For typical soliton comb generation with an external pump laser, it is crucial to start the sweep from short wavelength to long ones, in order to follow the thermal frequency drift of the ring on one hand, and on the other hand, to excite the resonance in a red detuned region, which is mandatory to generate soliton state [11]. In our experiment, when the pump begins to excite the resonance, a broad comb is generated with only primary lines, whose line spacing corresponds to 14 times the ring FSR. During this sweep, these primary lines gradually increase, while secondary lines (also called sub-combs) with a line spacing equal to the ring FSR grow around the primary lines. We have paused the pump wavelength scan at 1575.36 nm, that is when the sub-combs seem to merge. It leads to the broad comb measured in Fig. 5. The microresonator design provides anomalous Group Velocity Dispersion (GVD) (Fig. 4(a)) [6], which greatly facilitates Kerr comb generation. As shown on Fig. 5(a), the 30 dB bandwidth of the Kerr comb is measured to 13.6 THz (113 nm) containing 120 longitudinal modes. This broad bandwidth was achievable thanks to the association of i) the high power injected in the microresonator, ii) a high finesse for this microresonator (around 1500 in our case), and iii) a small anomalous GVD that we tried to design (Fig. 4(a)) [5]. These are the three key parameters to generate a broad Kerr comb [20]. At the difference with similar works based of the butt-coupling [6], [7], we test here the use of a single mode DFB laser as a gain chip [23]. The advantages are that it can be characterized as a standalone laser, and that the pump wavelength is easily tuned by adjusting the pump current. Moreover, the absence of side modes helps the optical self-locking of the laser frequency on a resonance frequency of the microring resonator [24]. During the acquisition of this optical spectrum, the electrical spectrum was also measured in the low and high frequency radio frequency (RF) domain, as shown the Fig. 5. On Fig. 5(b), one can notice a high RF noise below 500 MHz due to the relative intensity noise of the comb, which means the comb is not stable yet. This noise presents one broad peak at 155 MHz, and contribution of a much weaker peak around 310 MHz. These values are logically found again in the measurements of high frequency RF signals, as shown in Fig. 5(c). Indeed, we measured one broad peak at 113.5 GHz, with a 6.3-MHz-FWHM, with two sides lobes at 155 MHz from the central peak. Despite the clean shape of the optical comb spectrum, the broad central RF peak indicates the sub-combs previously mentioned have not perfectly merged. These broad peaks highlight the primary lines and therefore the sub-combs do not have a line spacing that is an exact multiple of the ring FSR. This comb measurement corresponds to a multiple mode-spaced (MMS) comb, as described in [25]. Moreover, as predicted by T. Herr *et al.* [25], our system has a ratio $\sqrt{\kappa/D_2} > 1$, which corroborates the hypothesis of MMS combs (κ is the total loss rate measured in Fig. 4(b), D_2 is linked to the resonator dispersion estimated from Fig. 4(a)). The shape of RF spectrum with three broad peaks reported in Fig. 5c) is very similar to the one obtained by T. Herr *et al.* [14]. Therefore, the comb of Fig. 5(c) may correspond to a comb formation state near a single soliton state [11], which would have presented a low RF noise at low frequency, and one narrow peak at 113.5 GHz. However, unlike these previously mentioned works, we didn't reach a single soliton state in this configuration. We explain this by the fact that we were not able here to correctly adjust the pump power and wavelength,

with the right combination of power and detuning, which leads to an unstable comb.

In Fig. 5(a), we observe reductions in the mode intensities at different locations: 1543 nm, 1564 nm, 1587 nm. By repeating these measurements, we concluded that the reason for such reductions was not instability, but a phenomenon already observed in a microresonator pumped by an external laser [26], namely mode crossings associated to the microresonator. Since our DFB laser emits a TE_{00} mode, we do believe these mode crossings are due to interactions between higher order spatial modes.

C. *Evolution of the Kerr frequency comb during a wavelength sweep*

We next investigate the stability of the Kerr comb during a pump wavelength sweep. To perform it, we detune the DFB pump from short to long wavelengths. This experiment was not stable with the microring used in subsection IV-B. Therefore, we use here a 200 µm microring with a 800×1500 nm^2 cross section and a 500 nm gap between the ring and the bus waveguide. The loaded quality factor is estimated to be $Q_l \approx 1.0 \times 10^6$, hence the injected power here is weaker than the one injected in the former microresonator.

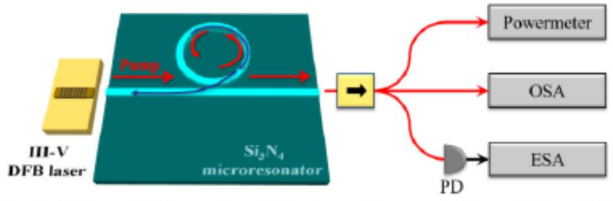

Fig. 6. Scheme of the experimental setup used to acquire the evolution of the Kerr comb during a slow pump wavelength sweep. The pump current source (ILX LDC-3742B) performs the sweep, while a powermeter measures the shape of the pumped resonance. An optical spectrum analyzer (OSA; Anritsu MS9740A) simultaneously records the comb generation. An electrical spectrum analyzer (ESA; Rohde & Schwarz FSU67) records the low frequency RF noise.

As schematized on Fig. 6, we acquire at the same time the output power, the optical spectrum and the electrical spectrum. However, unlike the previous observations of subsection IV.B where we reported a Kerr comb with a line spacing equal to the microring FSR, the output comb we measure here has a much broader FSR, i.e. 2.04 THz, that is out of our RF detection bandwidth. Thus, only the low frequency RF noise can be measured which is mandatory to distinguish an unstable comb like the one shown in the previous part, or a comb corresponding to a soliton state [12].

Fig. 7 reports the results of this experiment, which are quite different compared to previous works. Indeed in [7], [11], [27], when the pump wavelength gradually increases, the system undergoes a noisy state and generates a high noise modulation instability (MI) comb. Then, multiple low noise solitons steps are gradually generated in [11], or a self-locked regime is formed, followed by a single soliton step in [7], [27]. In our case, when the pump wavelength slightly increases, the transmission undergoes three states described in Fig. 7(a). After the initial state (I), the state (II) doesn't exhibit the MI comb, but an instable state. During this state, we assume the DFB laser undergoes a feedback from the resonator which gradually becomes stronger: such optical feedback modifies the dynamics of the DFB laser, which could become chaotic, as suggested from the observed broad RF noise in Fig. 7(c). Due to the averaging of the powermeter, the noise pattern is not captured and appears smooth in state (II) in Fig. 7(a). At state (III) the pump directly dives in the red region of the resonance, generating a low noise Kerr comb. It demonstrates a self-injection locking regime (similarly to [7]), where the pump wavelength is locked to the microring resonance despite its thermal shifting. Thus, as show the Fig. 7(b), the comb is very stable during the entire wavelength sweep corresponding to the zone (III). But, unlike previous works [7], [11], [27], the system does not reach the single soliton regime. Our case has been reported by M. Karpov *et al.* in [28] with a low pump power. Note that we also tuned the laser from long to short wavelength, and surprisingly the profile of the pumped (not shown here) of the resonance was similar, which confirms that self-injection locking compensates the thermal instabilities.

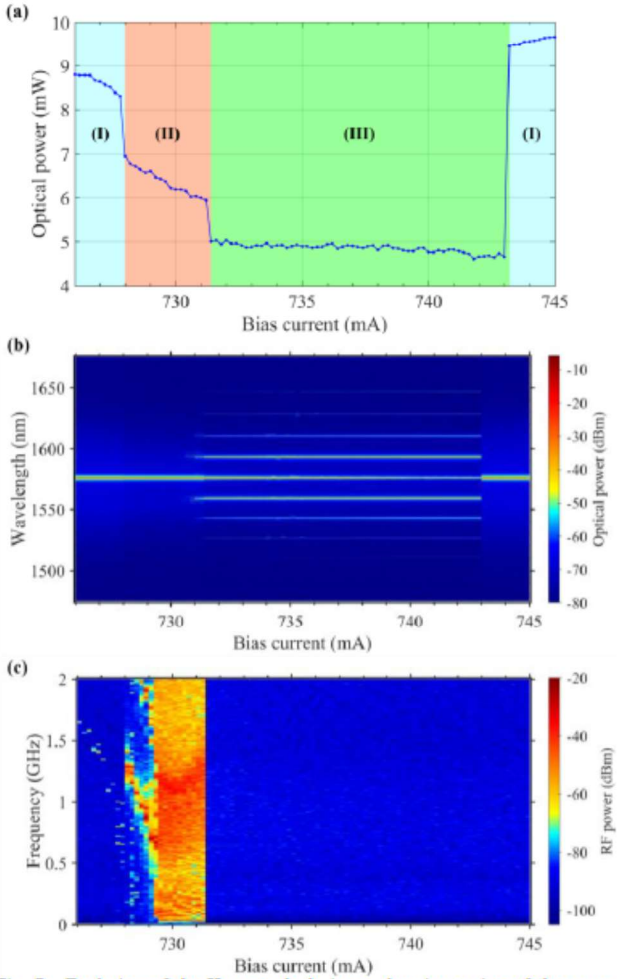

Fig. 7. Evolution of the Kerr comb during a slow increasing of the pump wavelength. (a) Transmission of the laser into resonance of the microresonator. (I) This state corresponds to the free running laser before the microring resonance. (II) This region is a very noisy unstable state with no Kerr comb generation. (III) This stable state corresponds to the low noise Kerr comb generation. Optical spectra (b) and electrical spectra (c) are measured for each current.

The comb measured in state (III) has a FSR corresponding to 17 times the microring FSR, and the electrical spectra in Fig. 7(c) show a persisting low noise. Moreover, by observing a spectrum in the zone (III) in Fig. 8(a), we can observe a typical $sech^2$ envelop, exception to the pump mode whose power is highly converted to the side bands during the FWM. It is worth mentioning that we didn't filter the pump mode in our measurements. In fact, the higher is the DFB current in the zone (III), the more the power at the pump wavelength is reduced, whereas the others lines of the comb gradually grow. One possible explanation to this unexpected behavior is that the increase of the pump provides nonlinear loss that adds to the initial linear loss of the resonator. During the pumping, the sum of these losses might reach the loss of the ring coupler, meaning a critical coupling of the resonator (thus a maximal extinction ratio of the resonance), which would explain the reduction of the pump line. In [28] and [29], a similar envelope is associated to a Perfect Soliton Crystal (PSC).

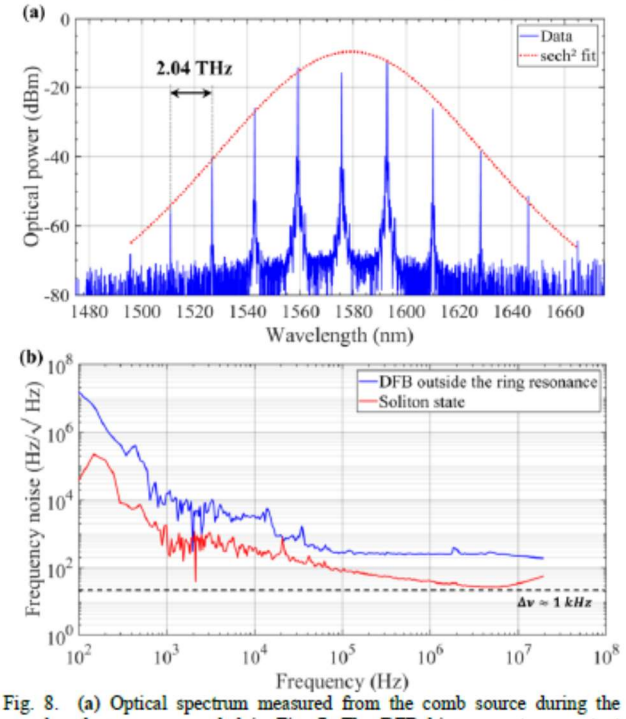

Fig. 8. (a) Optical spectrum measured from the comb source during the wavelength sweep proceeded in Fig. 7. The DFB bias current was set at 738.0 mA, meaning a 173-mW output power. Due to spurious losses (as discussed in Fig. 5), we estimate a maximum injection power of 133 mW. The line spacing is measured to be 2.04 THz. (b) Frequency noises of the signal acquired before the ring resonance (blue) and into the resonance (red), corresponding to the soliton state in (a).

From our measurements, we deduced that 17 evenly spaced optical pulses propagate in the microring. Moreover, the microresonator used here has a lower quality factor than the one employed in the previous part. Thus there is less power in the microresonator, which seems to be more favorable for the generation of PSC as mentioned by M. Karpov *et al.* in [28]. Furthermore, since our microresonators present avoided crossings between optical modes [26], it greatly increases the chance to generate a crystal soliton. This analysis confirms the locking of the system on one steady soliton power plateau during the state (III). Indeed, the wavelength sweep applied along the zone (III) should increase the detuning, and leads to other soliton steps until reaching the single soliton state, like the results of [11]. Since there is only one power plateau, it means that the effective detuning (i.e. the detuning between the DFB and the microring resonance) is constant and confirms the self-injection locking of the laser. Without further effective detuning, others soliton regimes cannot be reach. Consequently, the DFB ends out from microring resonance when its current increase is too high. The generated soliton depends of the initial couple of injected power and effective detuning. We assume that the high number of pulses propagating in the microring can be explained by the higher injected power compared to similar works [7]. Further theoretical investigation of the self-injection dynamics based on an adapted model like the one proposed by A. S. Voloshin and coworkers [30] may explain the behavior of our system. Others measurements, for instance, autocorrelation and amplitude noise measurements could also confirm the soliton regime [11], [12].

In order to evaluate the self-injection locking phenomena, we also performed optical linewidth measurement (Fig. 8b). Indeed, the self-injection locking phenomenon can greatly narrow the laser linewidth. By using a standard delayed self-heterodyne setup, we measured the Lorentzian linewidth at different steps of the DFB laser wavelength tuning. Outside the resonance (at region (I)), the linewidth free running laser is measured to 60 kHz. The region (II) is too unstable to perform a linewidth measurement. However, in the state (III), we measured a pump linewidth narrowed to 1 kHz, which actually corresponds to the lowest measurable linewidth with our setup and the available optical power.

V. CONCLUSION

We have developed a Si_3N_4/SiO_2 on silicon fabrication platform that allows the fabrication of high quality microresonators. We have demonstrated a compact optical frequency comb source formed by butt-coupling an InGaAsP/InP DFB laser with a Si_3N_4/SiO_2 microresonator. We succeed to generate a broad comb with a 30 dB bandwidth of 13.6 THz, which is one of the broadest measured for a 114 GHz FSR microresonator directly pump by a gain chip. Moreover, we measure the RF response at low and high frequency, exhibiting behavior similar to classical setup with a microresonator pumped by an external laser. Such performance on portable systems offers the potential for a wide variety of applications relying on stable frequency comb such as metrology, communications [3] or waveform generation [31].

The flexibility of our hybridization system, which permits to test different rings, allows to generate different combs. By pumping another microring, we have demonstrated a perfect soliton crystal, consisting in 17 optical pulses regularly spaced in the microring. Further works will investigate the conditions of soliton's appearance by measuring relevant parameters such as power threshold, pump detuning and comb frequency spacing variations. This should allow a better control of the solitonic regimes, which in turn will enable to target a large

number of various applications such as, e.g., ultra-fast ranging distance [2] or calibrations of astronomical spectrographs [32].

To improve our device, we now work on improving the mode matching between the two chips. It will facilitate the alignment and reduce the mains source of coupling loss, which is the main challenge in the butt-coupled devices. In addition, we work on the design of new microresonators in order to increase their quality factor. These two future improvements will reduce the comb generation threshold. Hence it should be possible to increase the optical length of the microresonator and use the generated frequency comb for microwave applications. To go further, the DFB laser and the microresonator could be assembled on a common platform, which will enhance the mechanical stability and yield a supplementary step toward an industrialization process. In order to control the pump optical phase, this assembly would also greatly beneficiate from a microheater that could be implemented on the top of the passive Si_3N_4 waveguides, as in [33].

ACKNOWLEDGMENT

The authors thank S. Guerber for stimulating discussions on dispersion simulations.

REFERENCES

[1] S. B. Papp *et al.*, "Microresonator frequency comb optical clock," *Optica*, vol. 1, no. 1, p. 10, 2014.

[2] P. Trocha *et al.*, "Ultrafast optical ranging using microresonator soliton frequency combs," *Science*, vol. 359, no. 6378, pp. 887–891, 2018.

[3] J. Pfeifle *et al.*, "Coherent terabit communications with microresonator Kerr frequency combs," *Nat. Photonics*, vol. 8, no. 5, pp. 375–380, 2014.

[4] W. Liang, D. Eliyahu, A. B. Matsko, V. S. Ilchenko, D. Seidel, and L. Maleki, "Spectrally pure RF photonic source based on a resonant optical hyper-parametric oscillator," *Laser Reson. Microresonators, Beam Control XVI*, vol. 8960, p. 896010, 2014.

[5] H. El Dirani *et al.*, "Annealing-free Si_3N_4 frequency combs for monolithic integration with Si photonics," 2019.

[6] B. Stern, X. Ji, Y. Okawachi, A. L. Gaeta, and M. Lipson, "Battery-operated integrated frequency comb generator," *Nature*, vol. 562, no. 7727, pp. 401–405, 2018.

[7] A. S. Raja *et al.*, "Electrically pumped photonic integrated soliton microcomb," *Nat. Commun.*, vol. 10, no. 1, pp. 1–8, 2019.

[8] Y. K. Chembo, "Kerr optical frequency combs: Theory, applications and perspectives," *Nanophotonics*, vol. 5, no. 2, pp. 214–230, 2016.

[9] X. Ji *et al.*, "Ultra-low-loss on-chip resonators with sub-milliwatt parametric oscillation threshold," *Optica*, vol. 4, no. 6, p. 619, 2017.

[10] T. J. Kippenberg, R. Holzwarth, and S. A. Diddams, "Microresonator-based optical frequency combs," *Science*, vol. 332, no. 6029, pp. 555–559, 2011.

[11] T. J. Kippenberg, A. L. Gaeta, M. Lipson, and M. L. Gorodetsky, "Dissipative Kerr solitons in optical microresonators," *Science*, vol. 361, no. 6402, 2018.

[12] A. L. Gaeta, M. Lipson, and T. J. Kippenberg, "Photonic-chip-based frequency combs," *Nat. Photonics*, vol. 13, no. 3, pp. 158–169, 2019.

[13] C. Lafforgue *et al.*, "Broadband supercontinuum generation in nitrogen-rich silicon nitride waveguides using a 300 mm industrial platform," *Photonics Res.*, vol. 8, no. 3, pp. 352–358, 2020.

[14] T. Herr *et al.*, "Temporal solitons in optical microresonators," *Nat. Photonics*, vol. 8, no. 2, pp. 145–152, 2014.

[15] V. Brasch, M. Geiselmann, M. H. P. Pfeiffer, and T. J. Kippenberg, "Bringing short-lived dissipative Kerr soliton states in microresonators into a steady state," *Opt. Express*, vol. 24, no. 25, pp. 29312–29320, 2016.

[16] M. Faugeron *et al.*, "High-power tunable dilute mode DFB laser with low RIN and narrow linewidth," *IEEE Photonics Technol. Lett.*, vol. 25, no. 1, pp. 7–10, 2013.

[17] H. El Dirani *et al.*, "Crack-free silicon-nitride-on-insulator nonlinear circuits for continuum generation in the c-band," *IEEE Photonics Technol. Lett.*, vol. 30, no. 4, pp. 355–358, 2018.

[18] L. Azarnouche *et al.*, "Benefits of plasma treatments on critical dimension control and line width roughness transfer during gate patterning," *J. Vac. Sci. Technol. B, Nanotechnol. Microelectron. Mater. Process. Meas. Phenom.*, vol. 31, no. 1, p. 012205, 2013.

[19] H. El Dirani *et al.*, "Ultralow-loss tightly confining Si_3N_4 waveguides and high-Q microresonators," *Opt. Express*, vol. 27, no. 21, pp. 30726–30740, 2019.

[20] S. Coen and M. Erkintalo, "Universal scaling laws of Kerr frequency combs," *Opt. Lett.*, vol. 38, no. 11, pp. 1790–1792, 2013.

[21] A. A. Savchenkov, A. B. Matsko, D. Strekalov, M. Mohageg, V. S. Ilchenko, and L. Maleki, "Low threshold optical oscillations in a whispering gallery mode CaF_2 resonator," *Phys. Rev. Lett.*, vol. 93, no. 24, pp. 2–5, 2004.

[22] N. M. Kondratiev *et al.*, "Self-injection locking of a laser diode to a high-Q WGM microresonator," *Opt. Express*, vol. 25, no. 23, pp. 28167–28178, 2017.

[23] S. Boust *et al.*, "Compact optical frequency comb source based on a DFB butt-coupled to a silicon nitride microring," in *2019 International Topical Meeting on Microwave Photonics (MWP)*. IEEE, 2019.

[24] A. A. Savchenkov *et al.*, "Self-injection locking efficiency of a UV Fabry – Perot laser diode," vol. 44, no. 17, pp. 4175–4178, 2019.

[25] T. Herr *et al.*, "Universal formation dynamics and noise of Kerr-frequency combs in microresonators," *Nat. Photonics*, vol. 6, no. 7, pp. 480–487, 2012.

[26] S. Ramelow *et al.*, "Strong polarization mode coupling in microresonators," *Opt. Lett.*, vol. 39, no. 17, pp. 5134–5137, 2014.

[27] N. G. Pavlov *et al.*, "Narrow-linewidth lasing and soliton Kerr microcombs with ordinary laser diodes," *Nat. Photonics*, vol. 12, no. 11, pp. 694–698, 2018.

[28] M. Karpov, M. H. P. Pfeiffer, H. Guo, W. Weng, J. Liu, and T. J. Kippenberg, "Dynamics of soliton crystals in optical microresonators," *Nat. Phys.*, vol. 15, no. 10, pp. 1071–1077, 2019.

[29] D. C. Cole, E. S. Lamb, P. Del'Haye, S. A. Diddams, and S. B. Papp, "Soliton crystals in Kerr resonators," *Nat. Photonics*, vol. 11, no. 10, pp. 671–676, 2017.

[30] A. S. Voloshin, J. Liu, N. M. Kondratiev, G. V. Lihachev, T. J. Kippenberg, and I. A. Bilenko, "Dynamics of soliton self-injection locking in a photonic chip-based microresonator," in *2020 Conference on Lasers and Electro-Optics (CLEO)*. IEEE, 2020.

[31] P. Ghelfi *et al.*, "A fully photonics-based coherent radar system," *Nature*, vol. 507, no. 7492, pp. 341–345, 2014.

[32] M.-G. Suh *et al.*, "Searching for Exoplanets Using a Microresonator Astrocomb," *Nat. Photonics*, vol. 13, no. 1, pp. 25–30, 2019.

[33] P. Primiani *et al.*, "Silicon Nitride Bragg Grating with Joule Thermal Tuning for External Cavity Lasers," *IEEE Photonics Technol. Lett.*, vol. 31, no. 12, pp. 983–986, 2019.

Sylvain Boust was born in Clamart, Paris, in 1993. He received his engineer's and master's degree from the Institut d'Optique Graduate School (IOGS), Saclay, France, in 2017. Since 2017, he pursues his Ph.D degree at III-V Lab, Palaiseau, France, and Institut FOTON, Rennes, France, on PICs based on the butt coupling between III-V and Si_3N_4 chips.

Houssein El Dirani was born in Bednayel, Lebanon, in 1993. He received the M.Sc. degree in optoelectronics from the National School of Physics, Electronics and Materials (Phelma), Grenoble, France, in 2016, and the Ph.D degree in 2019 from Lyon central school, Lyon, France for his doctoral research on the development of high quality silicon nitride chips for integrated nonlinear photonics. In 2019, he joined the process integration group of STMicroelectronics at Crolles (France), where he is currently working on BiCMOS technologies.

Laurène Youssef (https://orcid.org/0000-0003-0504-4398) was born in Lebanon in 1992. After completing her B.S. in general chemistry, she received M.S. degree in physical chemistry of materials from Lebanese University, Beirut, in 2015. Then she moved to France and obtained the double Ph.D. degree in physical chemistry and materials science from both

University of Montpellier, France and Lebanese University, Beirut, in 2018. Her field of study was centered on plasma deposition mechanisms.
From 2018 till present, she is a postdoctoral fellow researcher in Laboratoire des Technologies de la Microélectronique, a CNRS institute located in Grenoble, France and integrated to the site of CEA Leti. Her works are concentrated on developing plasma etching techniques of silicon and silicon nitride devices for photonics, nonlinear optics and quantum applications.
Dr. Youssef received two Excellence awards during her B.S. in 2013 and M.S. in 2015 and contributed to the conception of a prototype plasma reactor in Lebanese University during her PhD.

Alexandre Larrue received his engineering degree from ENSPG, and M.S degree from INPG, Grenoble, France, in 2006. He received his PhD degree from Université de Toulouse in 2009. During his PhD, he focused on the design, the fabrication and the characterization of photonic crystal laser sources. From 2010 to 2012, he was a postdoctoral fellow in the international joint lab CINTRA in Singapore, working on III-V nanowires. From 2012 to 2014, he was a Research fellow at LAAS-CNRS Toulouse, conducting research on GaSb-based laser diodes for optical spectroscopy. Since 2014, he is a research engineer in III-V Lab. His research interests include laser diodes, photonic integrated circuits, III-V material processing and advanced lithography for submicronic photonic structures.

Camille Petit-Etienne received her Ph.D degree in Process Engineering and High Technologies from Pierre et Marie Curie University in 2007, working on deposition of silicon oxide with plasma enhanced chemical vapor deposition (PECVD) at low pressure and atmospheric pressure on steel substrates for anti-corrosion application in the Laboratory of Plasma Processes Engineering and Surface Treatments at ENSCP.
In 2008, she was given a fixed-term contract at the Laboratoire des Technologies de la Microélectronique (LTM). This experimental work was performed in close collaboration with CEA-Leti, ST Microelectronics and Applied Materials, and consisted in the development of new plasma technologies (i.e. pulsed plasmas processes), using state of the art tools located in the CEA-Leti facilities. She became research engineer on permanent contract in 2011. At the LTM, Dr. Petit-Etienne is responsible of LTM plasma etching tools (200 and 300-mm industrial platforms) located in the CEA-Leti clean room and she still works on the development and optimization of new plasma processes of materials integrated in advanced CMOS devices, in silicon photonics technology and for photovoltaic applications.
Dr. Petit-Etienne is an organizing committee member of the Plasma Etch and Strip in Microelectronics (PESM) workshop since 2010.

Sébastien Kerdilès received the Ph.D degree in Materials Science from University of Caen, France, in 2000. Then, he worked 2 years as process engineer for X-ION, a start-up in Paris area, where he developed surface treatments using multi-charged ions beam. From 2002 to 2013, he works for SOITEC group as a research staff member first, then as technology development manager, and finally as SOI process and product designer. During this period, he contributed to the industrialization of 200 & 300 mm SOI substrates manufacturing, including RF-SOI and FD-SOI.
Since 2013, Dr. Kerdilès joined CEA-LETI, where he is in charge of thermal treatments engineering. His research interests include LPCVD of dielectrics and semiconductors, advanced substrates development and the investigation of pulsed laser annealing for various applications such as 3D integration and MEMS. He authored or co-authored more than 50 journal articles and conference papers, 1 book chapter and holds over 20 patents.

Erwine Pargon was born in Paris, France in 1977. She received *her M.S. in 2001 and Ph. D. in 2004* in Material Sciences, from the University of Grenoble-Alpes in France. From 2005 to 2006, she was a postdoctoral researcher at the Chemical Engineering department of UC Berkeley in USA. Since 2006, she is an associate researcher at the "Laboratoire des Technologies de la Microélectronique" (LTM), a joint academic unit of the CNRS and Grenoble Alpes University in Grenoble, located in the CEA/leti site in Grenoble, France. From 2019, she led the LTM etch team. Her research interest includes the development and characterization of plasma etching processes involved in the elaboration of advanced devices for microelectronic, photonics and photovoltaics applications. In particular, she worked on an important issue in plasma patterning, the pattern sidewalls roughness by proposing plasma strategies to minimize it or innovative metrology to measure it. She has co-authored more than 80 papers in peer-reviewed journals and has participated to about 30 invited talks at international conferences. In 2010, she was awarded the Bronze Medal of CNRS for her research achievements. She is a committee member of the "Advanced Etch Technology for Nanopatterning" conference of the SPIE since 2012, of the Plasma Etch and Strip in Microelectronics (PESM) workshop since 2013 and of the Plasma Science Technology Division of the AVS Symposium since 2017.

Mickaël Faugeron received his engineer diploma and PhD degree from Télécom Physique Strasbourg (Université de Strasbourg), and Ecole Supérieure d'Electricité (Supelec) in 2009 and 2012 respectively.
From 2012 and 2016 he was a Research Engineer at III-V Lab, Palaiseau (France), working on the design, fabrication, and characterization of high-power optoelectronic devices (DFB lasers, SOA, MOPA) on InP substrate, for microwave photonic applications and optical communications.
He joined Thales Alenia Space Research Department, Toulouse (France) in 2016, where his activities are now focused on the applications of photonic technologies in space, for on-board RF processing and free-space optical communications, and the evaluation of critical components and technologies.

Marc Vallet received the engineer diploma from the Institut d'Optique Graduate School, Orsay, France, in 1988, and the Ph.D. degree from Université Paris VI, France, in 1991, while working on nonlinear optics in Laboratoire Kastler Brossel. After a postdoctoral position at the University of Toronto, Canada, he joined in 1993 the University of Rennes, France. Since 2003, he has been a Professor of Physics, assigned to the Institut de Physique de Rennes until 2017, and has joined the Institut FOTON in 2017. His recent works, both basic and application-oriented, are focused on laser physics, nonlinear dynamics and linewidth stabilization for microwave photonics applications.

François Duport was born in Grenoble, France, in 1979. He received his engineering degree and DEA (Master of Science) in Optical Networks and Telecommunications from ENST de Bretagne, Brest, France, in 2002 and his PhD degree in physics field in November 2008 from the ENS de Cachan, France.
From 2002 to 2003, he was a Research Assistant with the IMT of Neuchâtel, working on the design of wavelength's tunable optical filters made with SOI MOEMS technology. From 2004 to 2007, he worked on the optic to microwave frequency conversion in a travelling-wave device by the mean of three waves mixing in electro-optic polymers. From 2007 to 2009, he was a Temporary Research and Teaching Assistant with the ESYCOM laboratory working on phototransistor and microwave photonic structures by the coupling of MOEMS technology and MSM photodiodes. From 2010 to 2015, he was a FNRS Postdoctoral Researcher with the ULB working on optical reservoir computers. His main achievements were the implementations of the first all optical reservoir computer and the first fully analog reservoir computer. Since 2016, he is a Research Engineer with the III-V lab, Palaiseau, France, working on lasers and SOA for microwave-photonic applications.

Corrado Sciancalepore received the M.S. degree in engineering physics from Politecnico di Torino, Italy, in 2009, and the Ph.D. degree in optical and electrical engineering from the École Centrale de Lyon, France, in 2012.
From 2012 to 2013, he was a Research Assistant with the Institute of Nanotechnology, based in Lyon, France. From 2014 until 2019, he was with the CEA-LETI, based in Grenoble, France, as a permanent researcher within the optics and photonics division. His research interests include the physics of optoelectronic devices, semiconductor lasers, nonlinear integrated optics, and silicon photonics. In 2020, he was hired by SOITEC, based in Bernin, France, as senior photonics material expert. He is the author of more than 80 articles and international conference proceedings, one book chapter, and holds six patents.
Dr. Sciancalepore was recipient of the IEEE Group IV Photonics Conference Best Paper Award in 2011.

Frédéric van Dijk was born in Chevreuse, France, in 1972. He received the Ph.D. degree from Université Paul Sabatier, Toulouse, France, in 1999. His study, performed at LAAS-CNRS, Toulouse, dealt with growth, process, and characterization of AlGaAs/GaAs VCSEL structures. In 2000, he joined Thales Research and Technology, Orsay, France. He is currently leading the "near infrared optronic devices" group within III-V Lab that is working on design, fabrication and characterization of III-V semiconductor laser sources, photodetectors and photonic integrated circuits covering the 700 nm to 1700 nm range for optical analog signal distribution, high speed data sampling, LIDAR systems, free-space optical transmissions, atomic clocks. He is in particular involved in studies on high power laser sources at 1.5 µm, and photonic integrated circuits for microwave and remote sensing